The Gaussian beam mode analysis of classical phase aberrations in diffraction-limited optical systems

INSTITUTE OF PHYSICS PUBLISHING EUROPEAN JOURNAL OF PHYSICS

Eur. J. Phys. **24** (2003) 403–412 PII: S0143-0807(03)57693-0

The Gaussian beam mode analysis of classical phase aberrations in diffraction-limited optical systems

Neil Trappe[1], **J Anthony Murphy**[1] **and Stafford Withington**[2]

[1] National University of Ireland, Maynooth, Co Kildare, Republic of Ireland
[2] Cavendish Laboratory, Madingley Road, Cambridge CB3 OHE, UK

E-mail: neal.a.trappe@may.ie

Received 23 December 2002, in final form 6 February 2003
Published 23 June 2003
Online at stacks.iop.org/EJP/24/403

Abstract

Gaussian beam mode analysis (GBMA) offers a more intuitive physical insight into how light beams evolve as they propagate than the conventional Fresnel diffraction integral approach. In this paper we illustrate that GBMA is a computationally efficient, alternative technique for tracing the evolution of a diffracting coherent beam. In previous papers we demonstrated the straightforward application of GBMA to the computation of the classical diffraction patterns associated with a range of standard apertures. In this paper we show how the GBMA technique can be expanded to investigate the effects of aberrations in the presence of diffraction by introducing the appropriate phase error term into the propagating quasi-optical beam. We compare our technique to the standard diffraction integral calculation for coma, astigmatism and spherical aberration, taking—for comparison—examples from the classic text '*Principles of Optics*' by Born and Wolf. We show the advantages of GBMA for allowing the defocusing of an aberrated image to be evaluated quickly, which is particularly important and useful for probing the consequences of astigmatism and spherical aberration.

(Some figures in this article are in colour only in the electronic version)

1. Introduction

The classical diffraction theory of aberrations is usually presented in terms of Fresnel diffraction integrals in advanced physics courses, as in '*Principles of Optics*' by Born and Wolf [1]. In the analytical technique presented below, propagating beams of coherent light can be considered to be composed of a linear sum of Gaussian beam modes (GBM) [2] in the paraxial limit (when Fresnel diffraction pertains). Re-synthesizing the beam at any plane by adding together

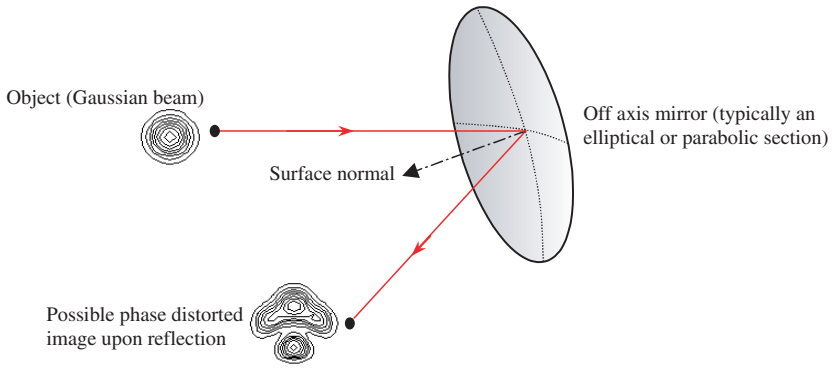

Figure 1. The image may be distorted after reflection from the off-axis mirror. A contour plot of the object and the image illustrates possible effects of phase distortion on beam quality.

the correct combination of modes allows us to gain valuable physical insight into the typical characteristics of diffraction, i.e. beam spreading and intensity pattern evolution. GBMs can also be traced very easily and very efficiently through a beam guide that consists of a line of focusing elements (lenses and mirrors). In a perfect non-aberrating beam guide, the modes maintain their character without distortion or scattering. The modes do, however, suffer order-dependent phase slippages with respect to each other as they propagate. This allows evolution in the shape of a complex optical beam which, in effect, consists of a combination of pure modes. GBMA enables diffraction patterns to be determined computationally without the need for any numerical integrations. Therefore, in the teaching of optics through computational physics, this approach offers a less intensive method. In this section we introduce a brief background to optical aberrations and how they were classified and analysed traditionally. In section 2 we present a simple alternative GBMA technique to the established methods for analysing such effects.

When non-ideal phase-transforming components are used in an optical system, a deterioration in the quality of any diffraction-limited images results (see figure 1). Perfect phase-transforming off-axis mirrors, for example, will suffer from such effects if the input field is defocused (for example, if the input object is longitudinally displaced in the system) [3]. Paraxial or Gaussian optics are only approximately correct in describing image formation and, in the derivation of paraxial equations, the approximations $\sin\delta \approx \delta$ and $\cos\delta \approx 1$ are made for small angles. This leads to normal perfect imaging, derived in elementary ray-tracing analysis. If the next term is considered in the expansion, then we have third-order theory, in which case $\sin\delta \approx \delta + \delta^3/3$ and $\cos\delta \approx 1 - \delta^2/2$ are the lowest-order terms. The aberrations that affect image quality are generally most important in the third-order approximation [4]. These aberrations have been classified by Ludwig von Seidel and are referred to as Seidel aberrations [6].

For coherent systems the phase errors due to the distorted wavefront can also be expanded in a series of Zernike polynomials [1]. Clearly, such aberrations will affect the phase front of a pure GBM, causing the modal power to be scattered into other modes and resulting in a distorted beam pattern. This then suffers shape evolution and is no longer a pure mode. In GBM theory, power scattering between adjacent modes can be used to measure the level of aberration introduced to the optical beam.

The departure from ideal diffraction-limited imaging is one of the principal consequences of such phase aberrations. To illustrate this, figure 2 shows two phase fronts at the exit pupil of an optical system: W1, which is perfectly spherical; and W2, which is an aberrated phase front (the figure follows the convention and notation used in [1]). The ideal spherical wavefront

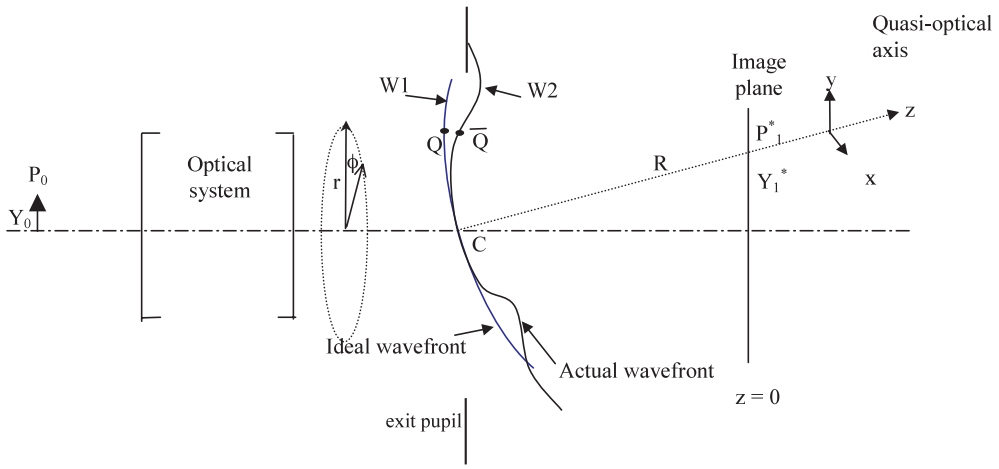

Figure 2. An illustration of aberration in terms of a Gaussian spherical wavefront.

produces a perfect diffraction-limited Airy spot at the image plane [5]. Wavefront W2 is an example of a more realistic wavefront, which is aspherical and whose shape represents the actual effect of the optical system.

The deformation of the real wavefront from the ideal wavefront is usually described by an aberration function, Φ. Consider figure 2, in which a monochromatic point source P_0 produces a perfect paraxial image at the point P_1^* at the image plane. We define the z-axis as lying along CP_1^*, where C is the centre of the exit pupil. The off-axis distances to the object point source P_0 and the image point P_1^* are represented by the off-axis distances Y_0 and Y_1^*, respectively. The intensity at an arbitrary point P in the vicinity of the image plane can be written (assuming $a/R \ll 1$, where a is the radius of the exit pupil and following [1]) as

$$i(p) = \frac{1}{\pi^2}\left|\int_0^1\int_0^{2\pi} \exp\left(\mathrm{i}\left(k\Phi - v\rho\cos(\phi-\psi) - \frac{1}{2}u\rho^2\right)\right)\rho\,\mathrm{d}\rho\,\mathrm{d}\phi\right|^2 \qquad (1)$$

where $u = \frac{2\pi}{\lambda}\left(\frac{a}{R}\right)^2 z$, $v = \frac{2\pi}{\lambda}\left(\frac{a}{R}\right)\sqrt{x^2+y^2}$, $\psi = \arctan(y/x)$, and x, y and z are co-ordinates *with respect to the perfect image point* (see figure 2). $\rho = r/a$ and ϕ define the cylindrical co-ordinates *at the exit pupil*. Note that this approximation is equivalent to Fresnel diffraction (i.e. paraxial propagation) if it is assumed that the effective optical axis of the system is now given by CP_1^* and that the angle made with the optical axis is small. Thus, the exit pupil is regarded as approximately perpendicular to the chief ray CP_1^*. The same approximations are made in the derivation of GBM (i.e. the Fresnel approximation) and therefore it should be possible to investigate the application of a modal approach to the propagation of aberrations and the formation of distorted diffraction-limited images.

The function Φ represents the appropriate phase error term (aberration function) at the exit pupil. A perfect image $i(p)$ has the form of the ideal diffraction pattern for a point source (i.e. an Airy pattern when $\Phi = 0$). For a non-perfect situation, Φ is given by the expansion

$$\Phi = \sum_{l,n,m} A'_{lmn} r^n \cos^m \phi, \qquad (2)$$

where A'_{lmn} is a constant and the lowest-order contributions can be expressed in terms of the Seidel coefficients.

These Seidel (or primary) aberrations are divided into five different categories, namely spherical aberration, coma, astigmatism, curvature of field, and distortion. An expression for each of the primary aberrations is given in table 1, taken from [6].

Table 1. The five primary Seidel aberration functions.

Type of aberration	Representation (Φ)
Spherical aberration	Br^4
Coma	$Fr^3\cos(\phi)$
Astigmatism	$Cr^2\cos^2(\phi)$
Curvature of field	Dr^2
Distortion	$Er\cos(\phi)$

The Seidel coefficients B, C, D, E and F associated with the different types of aberration describe the relative magnitude of the aberration. For the general case, we can write

$$\Phi = Br^4 + Fr^3\cos\phi + Cr^2\cos^2\phi + Dr^2 + Er\cos\phi. \tag{3}$$

Rather than a simple power series, the aberration function Φ can also be expanded in terms of a complete set of orthogonal circle polynomials, referred to as Zernike polynomials. Zernike polynomials have the advantage for coherent systems of being orthogonal over the unit circle and, in optimizing optical design, are useful in balancing aberrations to maximize the intensity at the Gaussian focus. A full description of the application of Zernike polynomials can be found in [1].

In section 2 we detail GBMA background theory and consider the details of applying GBMA to the image-forming qualities of a beam that suffers from various Seidel aberrations. In section 3 we apply the GBM theory to specific examples of primary aberrations and compare the results with classical diffraction integral predictions, as presented in [1].

2. GBM analysis of phase aberrations

In GBM theory a monochromatic coherent beam can be represented by a scalar field E that can be written as a linear sum of independently propagating modes Ψ_m. The field at any plane z is simply given by

$$E_0(r,\phi,z) = \sum A_m \Psi_m(r,\phi;\, W(z),\, R(z)), \tag{4}$$

where W and R are beam parameters that depend on z and A_m are the mode coefficients [7]. If the field E is known at some reference plane z_0, then the mode coefficients can be calculated using the appropriate overlap integral of the general form

$$A_m = \int\int E_0(r,\phi,z_0)\Psi_m^*(r,\phi;\, W(z_0),\, R(z_0))r\,\mathrm{d}r\,\mathrm{d}\phi. \tag{5}$$

For example, at the uniformly illuminated circular exit pupil of an optical system, the mode coefficients are given by equation (5) on setting $E_0(r,\phi,z_0)$ to be unity over the aperture area. To incorporate the Seidel phase aberrations into GBMA, it is most convenient to use the associated Laguerre Gaussian modes $\Psi_m = \Psi_{n\alpha}$ of the form

$$\Psi_{n,\alpha}(r,\phi;\, W(z),\, R(z)) = \sqrt{\frac{2(2-\delta_{0n})n!}{W(z)^2\pi(n+\alpha)!}}\left(\frac{2r^2}{W(z)^2}\right)^{\frac{\alpha}{2}} L_n^\alpha\left(\frac{2r^2}{W(z)^2}\right)\exp\left(-\frac{r^2}{W(z)^2}\right)$$
$$\times\ \exp\left(-\mathrm{j}k\left(\frac{r^2}{2R(z)}\right)\right)\exp(\mathrm{j}(2n+\alpha+1)\Delta\phi_{00}(z))\exp(\mathrm{j}\alpha\phi), \tag{6}$$

where $L_n^\alpha(x)$ are the associated Laguerre polynomials of order n and degree α [8]. The beam radius, $W(z)$ (or *beam-width parameter*), and the phase-front radius of curvature, $R(z)$, are functions of distance z and are given respectively by

$$W^2(z) = W_0^2\left[1+\left(\frac{z\lambda}{\pi W_0^2}\right)^2\right], \qquad \text{and} \qquad R(z) = z\left[1+\left(\frac{\pi W_0^2}{\lambda z}\right)^2\right], \tag{7}$$

where λ is the wavelength of the radiation and W_0 is the minimum value of W, which occurs at $z = 0$ and is referred to as the waist position. The value of W_0 is usually chosen to maximize the power in the fundamental mode [7]. In this way, the fundamental mode can be used as a zeroth-order approximation to the intensity distribution, and W gives the scale-size of the beam. In such a description, the waist will coincide with a focus. These modes, $\Psi_{n,\alpha}$, will propagate through an optical system without scattering and the output field at the image plane can be reconstructed by resuming the modes as in [2].

If it is assumed that phase aberration is now introduced into the propagating beam at some particular plane z', then we can relate the input beam,

$$E_{\text{in}}(r, \phi, z') = \Sigma A_m \Psi_m(r, \phi; W, R), \tag{8}$$

to the aberrated output beam $E_{\text{out}}(r, \phi, z') = E_{\text{in}}(r, \phi, z') \exp(\text{i}k\Phi(r, \phi))$. The effect of the phase error term can be determined by recalculating the true mode coefficients of the output beam using

$$B_m = \int_0^{r=a} \int_0^{\phi=2\pi} \{E_{\text{out}}(r, \phi)\} \Psi_m^* r \, \text{d}r \, \text{d}\phi = \int_0^{r=a} \int_0^{\phi=2\pi} \{E_{\text{in}}(r, \phi) \exp(\text{i}k\Phi)\} \Psi_m^* r \, \text{d}r \, \text{d}\phi. \tag{9}$$

This is computationally efficient, although equation (9) does not emphasize the modal scattering introduced by the aberrations. An alternative viewpoint is to regard the component modes as being distorted and scattered. Thus

$$E_{\text{out}}(r, \phi, z') = \Sigma A_m \{\Psi_m(r, \phi; W, R)\}^{\text{Distorted}} = \Sigma A_m \{\Psi_m(r, \phi; W, R) \exp(\text{i}k\Phi(r, \phi))\}. \tag{10}$$

Clearly, the distorted modal field $\Psi_m^D = \Psi_m \exp(\text{i}k\Phi(r, \phi))$ is no longer a true mode, but can itself be represented as a sum of true modes

$$\Psi_m^{\text{Distorted}} = \Psi_m \exp(\text{i}k\Phi(r, \phi)) = \sum S_{mm'} \Psi_{m'}. \tag{11}$$

$S_{mm'}$ can be thought of as elements of a scattering matrix responsible for describing the aberrating effects introduced into the general beam mode set. These elements are given by

$$S_{mm'} = \int \Psi_m(r, \phi) \exp[\text{i}k\Phi(r, \phi)] \Psi_{m'}^*(r, \phi) r \, \text{d}r \, \text{d}\phi. \tag{12}$$

The output field mode coefficients, B_m, are now given by $B_m = \Sigma S_{mm'} A_{m'}$. This approach is more computationally intensive, as a much larger number of integrations is required. However, clearly the $S_{mm'}$ are input-field independent and describe the aberrating effect of the optical system on the basis set of GBMs themselves (rather than the particular combination that makes up the input field). Thus, if the scattering matrix for a given aberrating optical system is known, then the effect on a range of fields (i.e. the appropriate B_m) can quickly be calculated.

GBMs are particularly powerful when examining the fields not just on the image plane (Fourier plane of the exit pupil) but also at other planes in the vicinity. This is particularly useful when it comes to examining images that suffer from spherical aberration and astigmatism. Away from the image plane, the beam is of course still expressed as a modal sum, $E(r, \phi) = \Sigma B_m \Psi_m(r, \phi; W, R)$. The width of the beam, W, scales accordingly with distance z away from the image plane, and the modes suffer relative phase shifts that result in changes in the beam shape.

The dimensionless 'optical parameters' u and v that are used in equation (1) relate the displacements (with respect to an origin at the perfect image point) along the longitudinal z-axis (u) and on the transverse (x, y)-plane (v). The relationships between u and v and the (x, y, z) displacements can, interestingly, be rewritten in terms of the parameters of the component GBMs (beam-width W and the phase-slippage term $\Delta\phi_{00}$ [7]). Assuming a modal waist of beam width W_0 at the paraxial image point, the phase-slippage parameter for propagation at distance z away is given by [2]

$$\Delta\phi_{00} = \tan^{-1}\left(\frac{\lambda z}{\pi W_0^2}\right). \tag{13}$$

This phase-slippage parameter reduces to $\pi/2$ as the distance z becomes large (if, for example, the exit pupil is in the far-field of the perfect image plane). In that case, the relationship between beam-width parameters at the image and the exit pupil, W_{EP} and W_0, are given by

$$W_0 = \frac{\lambda R}{\pi W_{\mathrm{EP}}}, \tag{14}$$

where R is the phase radius of curvature at the exit pupil. Thus, it can easily be shown that the relationship between u and the phase slippage is

$$u = \tan(\Delta\phi_{00})\left(\frac{a}{W_{\mathrm{EP}}}\right)^2. \tag{15}$$

This is a convenient relationship when expressing the variation of the intensity pattern with displacement u away from the image plane. A Fourier transformation of the exit pupil field is appropriate when the exit pupil is in the far-field of the image plane. When the exit pupil is in the near-field (sometimes the case in long-wavelength far-infrared quasi-optical systems) the situation is more complicated, as the true image plane does not coincide with the beam-waist position.

3. Examples

In this section we compare examples analysed using classical diffraction integrals with the corresponding results computed using GBMA. Three specific classical aberration types are analysed: coma, astigmatism and spherical aberration. The aberration function Φ in each case is taken for the examples presented in [1] *(Chapter IX 'The diffraction theory of aberrations')*.

3.1. Coma

To illustrate GBMA applied to classical coma, the phase term is introduced at the uniformly illuminated exit pupil of the system (uniform top-hat field) and then this field is propagated to the Fourier image plane to observe the effect. We can apply equation (9) to calculate the appropriate mode coefficients. Figure 3 illustrates how the reconstructed aberrated beam appears at the image plane. Since the exit pupil is uniformly illuminated, E_0 is taken to be a constant for the input field. The scales on the horizontal and vertical axes are expressed in terms of v_x and v_y, as in [1], and $u = 0$ at the image plane.

The coma term is set to $\Phi = 1.4(r^3 - 2/3r)\cos\phi$ to compare with results for the resulting aberration image presented in [1] (figure 9.6(b)). Mode coefficients corresponding to Laguerre Gaussian modes $\Psi_{n\alpha}$ (equation (6) above) up to order $n = 40$ and degree $\alpha = 4$ are used in the final summation to guarantee a high level of convergence. The parameters in this particular example were $a = 3.3\lambda$ and $R = 66.7\lambda$, where λ is the wavelength. The beam-width parameter at the exit pupil, W_{EP}, in the GBMA was $W_{\mathrm{EP}} = 0.7a$. The beam is then propagated to the image plane, causing a modal phase slippage of $\Delta\phi_{n\alpha} = (2n + \alpha + 1)\pi/2$. The overall shape of the comatic field that is reproduced by using GMBA agrees well with that of [1] (figure 3(a) above). The characteristic coma shape is also illustrated in the 3D plots.

3.2. Astigmatism

As a second example, we introduce an astigmatic phase error to a beam and compare the beam at the image plane with the result presented in [1] using the classical diffraction integral (equation (1)). Astigmatism arises when an object point lies an appreciable distance from the axis of symmetry, causing any incident cone of rays to strike the entrance pupil (e.g. mirror) asymmetrically [9].

For the GBMA of astigmatism, the phase term is again introduced at the exit pupil of the system (to a uniform top-hat field, as in the previous example of coma) and then this field is

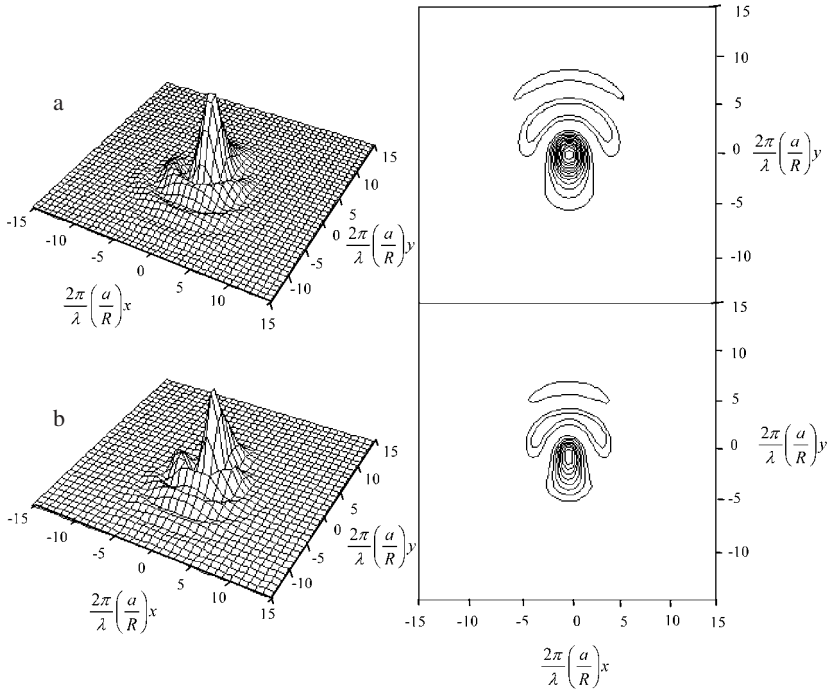

Figure 3. The image of the pupil plane for comatic aberration (a) plotted using a diffraction integral approach (equation (1)) and (b) reproduced using GBMA. The aberration function that is included is of the form $\Phi = 1.4\lambda(r^3 - 2/3r)\cos\phi$. Ten linear contour levels are used. The same area is plotted for cases (a) and (b).

propagated to the Fourier image plane to observe the aberrated image. As described in table 1, to include astigmatism a phase error term of the form $\exp(\mathrm{i}\alpha r^2\cos^2\phi)$ is introduced. Thus, the coefficients of the uniform field illumination of the exit pupil are given by

$$B_m = \int_0^{r=a}\int_0^{\phi=2\pi} E_{\mathrm{in}}\exp(\mathrm{i}\alpha r^2\cos^2(\phi))\Psi_m r\,\mathrm{d}r\,\mathrm{d}\phi. \tag{16}$$

The example of an astigmatic beam, taken from [1] (figure 9.9(b)), is reproduced in both 3D and as a contour plot. This is illustrated in figure 4, where the aberration function is given by $\Phi = 0.64\lambda r^2\cos(2\phi)$, along with the equivalent field, calculated using GBMA. The same aberrated characteristics are clearly extremely well reproduced in the GBM-reconstructed field, as in the field obtained by applying diffraction integrals. The input parameters were the same as for the coma example, i.e. input beam radius $W = 0.7a$ using Laguerre Gaussian modes $\Psi_{n\alpha}$ (equation (6)) of order $n = 40$ and degree $\alpha = 4$.

The main advantage of the GBM technique is that, once the coefficients for the aberrated field are calculated, the image can readily be investigated in the region around the nominal image plane. The output field can be calculated at any plane simply without any additional integrations (unlike the diffraction integral method) by resuming the Laguerre Gaussian modal sum and incorporating the appropriate W, R and $\Delta\phi_{n\alpha}$ [2]. Figure 5 illustrates the evolution of the astigmatic beam to two symmetrically displaced planes on either side of the image plane. Between the exit pupil and the image plane, $u = 0$, the appropriate phase slippage for the modes is given by $\Delta\phi_{n\alpha} = (2n + \alpha + 1)\pi/2$, since $\Delta\phi_{00} = \pi/2$.

Figures 5(a) and (c) show the field at planes where u is ± 10. This corresponds to phase slippages of $\Delta\phi_{00} = \pi/4$ and $3\pi/4$, respectively, from the exit pupil (or $\Delta\phi_{00} = \pm\pi/4$ from the image plane). In figure 5(a) the astigmatism is worse in the sagittal plane (tangential

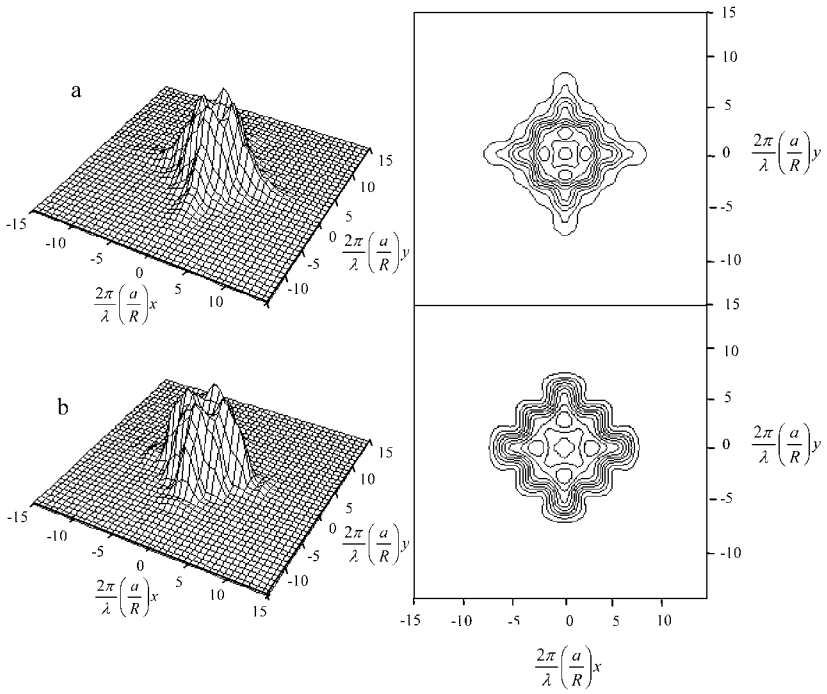

Figure 4. (a) The image of the pupil plane for astigmatic aberration, plotted using equation (1) as in Born and Wolf, and (b) reproduced using GBMA. The aberration function is of the form $\Phi = 0.64\lambda r^2 \cos 2\phi$. Ten linear contour levels are used. The same area is plotted for cases (a) and (b).

best focus) and in figure 5(c) the tangential component of the field is aberrated more severely (sagittal best focus). As expected, the best overall image is formed in between these cases, where the overall beam has the best focus (the circle of least confusion).

3.3. Spherical aberration

As outlined in table 1, the expression for spherical aberration ($\Phi \propto r^4$) is independent of ϕ and therefore has rotational symmetry about the optical axis. In an optical system, spherical aberration occurs when paraxial and non-paraxial rays do not converge to a common point focus (for example, for a single parabolic mirror). The more off-axis rays form an image closer to the exit pupil than the more paraxial geometric rays, so the image becomes spread out along the axis, as all rays are not brought to the same focus. The outer rays, which define the beam envelope, are referred to optically as the caustic surface.

Following the approach of previous examples, we can express an aberrated field at the exit pupil in terms of the modal coefficients given by

$$B_m = \int_0^{r=a} \int_0^{\phi=2\pi} E_0(r, \phi) \exp(\mathrm{i}\alpha k r^4) \Psi_m(r, \phi) r \, \mathrm{d}r \, \mathrm{d}\phi. \tag{17}$$

In reality, the use of the parabolic approximation for the phase curvature terms in paraxial imaging systems also introduces phase errors of the order of r^4. This also applies to the approximations made in [1] in the derivation of equation (1). However, in terms of an optical system, if we assume that the modes have true spherical wavefronts, then the effect of a perfect lens/mirror is to match exactly the phase curvature of the input and output modes. No errors in phase curvature due to the parabolic approximation should therefore occur in the case of a

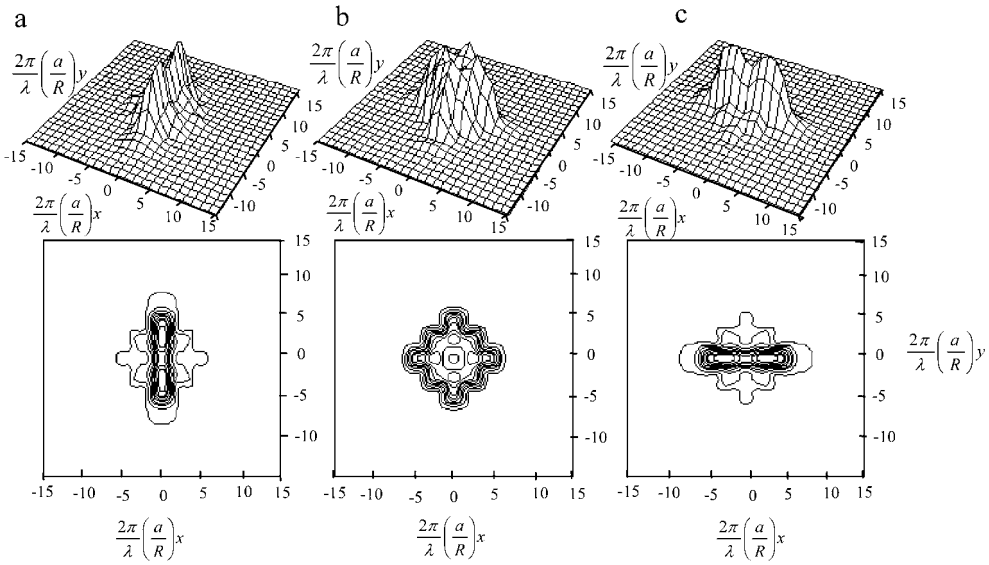

Figure 5. An astigmatic beam plotted (a) before the image plane, (b) at the image plane (cf figure 4) and (c) after propagation through the image plane. The GBM technique of including phase aberrations allows the beam to be plotted at any plane, once the appropriate mode coefficients are calculated.

perfect imaging system. If spherical aberration is present, then we assume that its effect on terms in r^4 dominates over the neglected terms in the parabolic approximation.

To illustrate the effect of spherical aberration, the image of a uniformly illuminated output pupil plane is plotted in the axial region of the image (Fourier) plane, following similar plots produced in [1]. A contour plot of the intensity variation around the image plane ($\pm z$) is shown in figure 6, computed using the GBM technique and based instead on the diffraction integral described in equation (1). This plot is equivalent to a figure that illustrates spherical aberration ($\Phi = 0.48\lambda r^4$) at optical wavelengths given by Born and Wolf [1] (figure 9.3).

The isophotes (the lines joining points of equal intensity) are shown in the region of the image between $u = \pm 40$, where z is set equal to zero at the image plane, to observe the effect of spherical aberration. The GBM modal technique reproduces very well the effects seen in the field produced using equation (1) and is, of course, much less computationally demanding. The same beam characteristics are again used as in the optical wavelength example that is presented in [1].

4. Discussion and conclusion

We have shown that it is possible to include the effect of the primary aberrations in a quasi-optical beam by introducing the appropriate phase error term into the calculation of the Gaussian mode coefficients. The main advantage of the GBMA technique over the diffraction integral method is its powerful ability to reproduce easily the beam pattern evolution in the vicinity of the image plane. Specific examples of astigmatism and spherical aberration were chosen to illustrate this. We have shown that, once the coefficients are calculated at the exit pupil of the system, the field can be reconstructed at any plane (including the near-field) by re-summing the appropriate Laguerre Gaussian modes in a process. This is less computationally demanding than traditional diffraction integral techniques.

One possible practical application of this straightforward GMB technique is in the inclusion of aberrations at real optical components in long-wavelength quasi-optical systems,

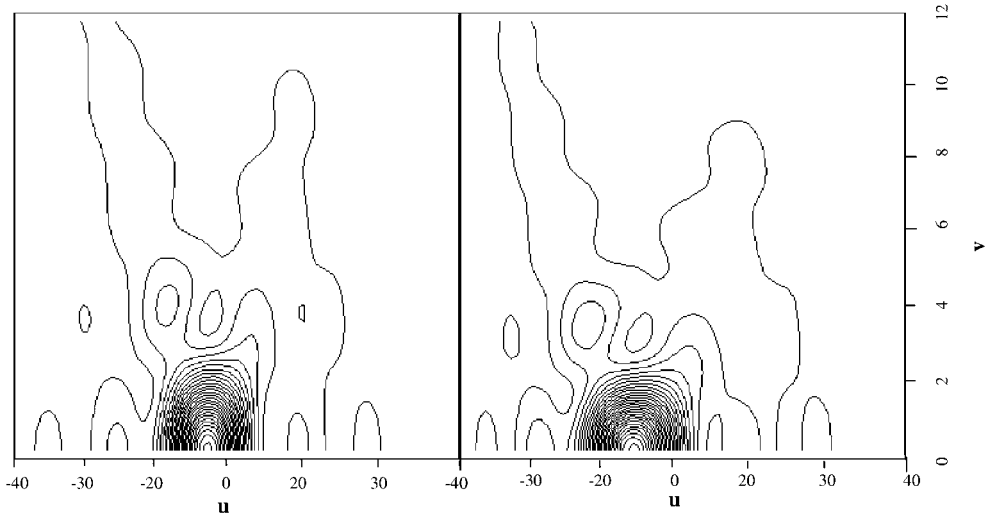

Figure 6. Spherical aberration produced in the vicinity of the image plane using (a) the diffraction integral technique and (b) the GBM technique.

if one has knowledge of the corresponding Seidel coefficients. The use of alternative physical optics techniques to analyse the distorting effect of an off-axis focusing mirror, for example, proves to be computationally intensive, because of the large number of integrals that need to be calculated [10], especially for optically large components [11]. The direct use of GBMA in analysing the aberrating effect of such off-axis systems also proves to be computationally difficult [10]. On the other hand, commercial ray-tracing packages can be used to extract each of the Seidel coefficients associated with any typical optical component. Having used the well-understood ray-tracing technique to obtain an expression for the aberrating effect of any mirror, the appropriate aberration function can be introduced into a quasi-optical beam using the GBMA approach described in this paper.

Acknowledgments

The authors wish to acknowledge the financial assistance of Enterprise Ireland and also the funding received by Neil Trappe from NUI Maynooth through the Daniel O'Connell Fellowship.

References

[1] Born M and Wolf E 1987 *Principles of Optics* 6th edn (New York: Pergamon)
[2] Murphy J A and Egan A 1993 Examples of Fresnel diffraction using Gaussian modes *Eur. J. Phys.* **14** 121–7
[3] Murphy J A 1987 Distortion of a simple Gaussian beam on reflection from off axis ellipsoidal mirrors *Int. J. Infrared Millim. Waves* **8** 1165
[4] Wilson R N 1996 *Reflecting Telescope Optics (Astronomics and Astrophysics Library)* vol 1 (New York: Springer)
[5] Hecht E 1998 *Optics* 3rd edn (New York: Addison-Wesley)
[6] Pedrotti F and Pedrotti L 1993 *Introduction to Optics* 2nd edn (Englewood Cliffs, NJ: Prentice-Hall)
[7] Goldsmith P F 1998 *Quasi-Optical Systems: Gaussian Beam Quasi-Optical Propagation and Applications* (Piscataway, NJ: IEEE)
[8] Martin D and Bowen J 1993 Long wave optics *IEE Trans. Microw. Theory Tech.* **41** 1676–89
[9] Jenkins F and White E 1957 *Fundamentals of Optics* 3rd edn (New York: McGraw-Hill)
[10] Withington S, Murphy J A and Isaak K G 1995 Representation of mirrors in beam-waveguides as inclined phase-transforming surfaces *Infrared Phys. Technol.* **36** 723–34
[11] O'Sullivan C, Murphy J A, Withington S, Ghassan Y, Atad-Ettedgui E, Duncan W, Henry D, Trappe N, Jellema W and van de Stadt H 2002 Far-infrared optics design and verification *Int. J. Infrared Millim. Waves* **23** 1029–45